Electrospinning Nonwovens of Polyacrylonitrile / synthetic Na-Montmorillonite Composite Nanofibers

Sliman Almuhamed, Magali Bonne, Nabyl Khenoussi, Jocelyne Brendle, Laurence Schacher, Bénédicte Lebeau, Dominique Adolphe

Electrospinning Nonwovens of Polyacrylonitrile / synthetic Na-Montmorillonite Composite Nanofibers

Sliman Almuhamed[*a], Magali Bonne[b], Nabyl Khenoussi[a], Jocelyne Brendle*[b], Laurence Schacher*[a], Bénédicte Lebeau[b], Dominique C. Adolphe[a]

[a] *Laboratoire de Physique et Mécanique Textiles EA 4365 UHA, ENSISA, 11 rue Alfred Werner F-68093 Mulhouse Cedex France.*

[b] *Université de Haute Alsace (UHA), CNRS, Pôle Matériaux à Porosité Contrôlée (MPC), Institut de Science des Matériaux de Mulhouse (IS2M), UMR 7361, F-68093 Mulhouse cedex, France.*

**Corresponding authors : jocelyne.brendle@uha.fr, laurence.schacher@uha.fr*

Abstract

Nonwovens of polymer/clay composite nanofibers (namely, Polyacrylonitrile/Na-montmorillonite, PAN/Na-MMT) are produced by electrospinning a solution of PAN in dimethylformamide containing synthetic Na-MMT. The influence of both Na-MMT amount and applied voltage on the properties of electrospun composite nonwovens was studied. Scanning electron microscopy (SEM), X-ray diffraction (XRD) thermogravimetric analysis (TGA-DTA), were used to evaluate the morphology, structure and thermal properties of composite nanofibers. SEM observations revealed that increasing the amount of Na-MMT in the solution or the applied voltage increases the average diameter of electrospun composite nanofibers. The prepared composite showed a higher thermal stability that the pristine PAN nanofibers. It was proven that the ion exchange properties of Na-MMT were maintained in the obtained composite.

Keywords: Electrospinning, Polyacrylonitrile, Montmorillonite, Composite nanofibers, Ion-substitution

1. INTRODUCTION

Electrospun nanofibers have been used in a variety and a wide range of applications including sensors, tissue engineering, wound dressing, filtration, fuel cell, capacitors, etc. [1–7] However, such applications require tailoring of the chemical composition, hydrophobicity, nanofiber surface porosity. Incorporation of fillers into the electrospun nanofibers has been recently used to prepare composite nanofibers since it is an economic, easy and effective way to introduce functionality into the electrospun nanofibers [8–12]. Depending on the nanofillers geometric shape, one can distinguish three categories of nanomaterials: spherical (e.g. metal or metal oxide nanoparticles[13,14]), fiber-like (e.g. carbon nanotubes or metal nanowires [15,16]) and platelet-like nanomaterials (e.g. natural or synthetic layered silicate [17]).

The commonly layered silicates used in preparing polymer/clay composites belong to 2:1 phyllosilicates having ion exchange properties (e.g. Na-montmorillonite). Their structure is composed of one sheet of alumina octahedron sandwiched and edge-shared with two sheets of silica tetrahedrons. The layers are over stacked and held together by van der Waals forces leading to forming gaps between the layers called the interlayer space or gallery. Owing to isomorphic substitution within the sheets (for example; Al^{3+} replaced by Fe^{2+} or Mg^{2+}, or Mg^{2+} replaced by Li^{+}), negative charges are generated and counterbalanced by cations that are located in the interlayer space [17].

Exfoliation of the silicate layers into the polymer matrix was found to be a promising approach to enhance mechanical and thermal properties of the produced electrospun nanocomposite [18–21]. However, complete exfoliation of silicate layers into the

electrospun polymer matrix leads to loose the interlayer space. Consequently, the loss of clay porosity renders such hybrid nanofibers inutile for applications requiring porosity of nanofiber.

In this paper, the incorporation of Na-montmorillonite (Na-MMT) layered silicate into polyacrylonitrile nanofibers in one step by electrospinning is reported. The effect of incorporating Na-MMT on the morphology and thermal properties of produced composite nanofibers and the influence of electrospinning process on the crystallographic structure of Na-MMT were investigated. The accessibility to the interlayer space of incorporated Na-MMT is also investigated.

2. MATERIALS AND METHODS

2.1. Synthesis of Na-Montmorillonite

Sodium acetate ($NaCOOCH_3$, 99%; Fluka, Saint-Quentin Fallavier, France), Pseudo-boehmite (Al_2O_3, 75%–78%, Pural SB1, Condea, Hambourg, Germany), Magnesium acetate tetra hydrate [$Mg(COO\ CH_3)_2 \bullet 4H_2O$ Fluka, Saint-Quentin Fallavier, France], Silica (SiO_2, 99.5%, Aerosil 130; Degussa, Evonik, Rheinfeld, Germany), Distilled water (H_2O), were used as received. Hydrofluoric acid (HF, 40 %; BDH) was diluted in order to obtain a 5wt% aqueous solution.

Na-montmorillonite having the following theoretical formula per half a unit cell: $Na_{0.4}(Al_{1.6}Mg_{0.4})(Si)_4O_{10}(OH,F)_2$ was synthesized according to Reinholdt et al. [22]. 0.412 g of $Na(CH_3COO)$, 1.076 g of $Mg(CH_3COO)_2 \bullet 4H_2O$, 1.302 g of Al_2O_3, 3 g of SiO_2 and 0.994 g of HF were added to 84.3 g of distilled water. After an aging step under stirring at room temperature for 2h, the hydrogel was transferred into a teflon-lined stainless steel autoclave and put in an oven at 220 °C for 72 h. After crystallization, the sample was

recovered by filtration, thoroughly washed with distilled water and dried at 60 °C overnight. The obtained sample is labelled Na-MMT.

2.2. Preparing solutions for electrospinning

Polyacrylonitrile (PAN) with molecular weight Mw = 150,000 $g.mol^{-1}$ purchased from Sigma-Aldrich (France) and pure N,N-dimethylformamide (DMF) (impurities less than 152 ppm in which water is less than 50 ppm) purchased from Fisher Scientific (France), were used as received.

Three suspensions of Na-MMT in DMF with a loading of 2, 3 and 5 wt% (with respect to the weight of the final charged solution) were prepared by mixing separately 0.44, 0.66 and 1.37 g of Na-MMT powder to 20 ml DMF using a high shear homogenizer from IKA (France) at 18,000 rpm during 30 min. The suspensions were ultrasonicated using an ultrasonic bath (Elmasonic S) with a frequency of 37 kHz for 30 min at 50 °C.

2.63, 2.66 and 2.73 g of PAN powder were then mixed to the prepared 2,3 and 5 wt% dispersions, respectively to obtain 12 wt% PAN solution loaded with 2, 3 or 5 wt% Na-MMT. The resulting suspensions were stirred for 24 h at 70 °C prior electospinning to insure the homogeneity of the final spinning charged solutions. PAN/Na-MMT composite nanofibers with 14.3, 20 and 29.4 wt% of Na-MMWT are expected.

To prepare pure PAN 12 wt% solution, 2.57 g of PAN powder was mixed to 20 ml DMF and stirred for 24 h at 70 °C prior electospinning.

2.3. Electrospinning conditions

The prepared PAN/Na-MMT and PAN solutions were electrospun by means of a home-made electrospinning set-up, illustrated schematically in Figure 1.

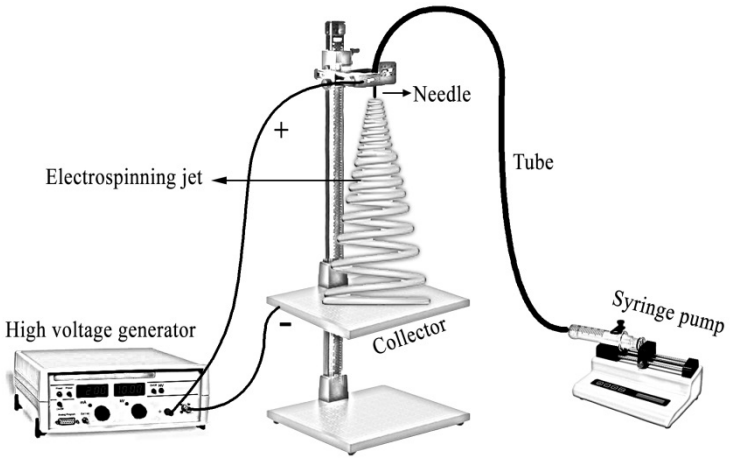

Figure 1 Scheme of the home-made Electrospinning setup

This set-up is based on the vertical projection of polymeric solution. A 20 ml syringe containing the solution is mounted on a pump. This latter feeds the solution through a tube of polyethylene to the tip of a needle connected to the positive output of a high voltage generator. The electrospinning process is carried out between the tip of the needle and a grounded plate of Teflon charged by graphite. PAN and PAN/Na-MMT solutions were all electrospun under the same ambient conditions of 21 ± 2 °C and 23 ± 2 % RH and the same process conditions by holding the distance between the tip of the needle and the collector at 20 cm and the feed-rate at 0.212 $ml.h^{-1}$ but varying the applied voltage (11.5, 13 and 14.5 kV).

2.4. Characterization of materials

The morphology of pristine and charged PAN nonwovens produced was characterized by scanning electron microscopy (Philips XL30 FEG). Prior analysis all samples were gold-coated in order to render their surface conductive for SEM purposes. Diameter of electrospun PAN and PAN/Na-MMT nanofibers were evaluated using Image J 1.45S software. In total, the diameter of 90 different nanofibers of each specimen was measured. A wide angle X-ray diffraction (WAXD) analysis was carried out using PANalytical X'Pert PRO MPD X-ray diffractometer at a scanning step of 0.02° in a 2θ range of 2-70°

for Na-MMT, PAN and charged PAN nonwovens. The wavelength of the X-ray beam was 0.154 nm (Cu k_α radiation).

Thermo-gravimetric analyses were performed by using a TG-DTA (SETARAM) apparatus. Approximately 10 mg of each sample were heated under an air flow (20 $mL.min^{-1}$ of N_2 and 5 $mL.min^{-1}$ of O_2) from 25 °C to 800 °C at a heating rate of 5 $°C.min^{-1}$.

2.5. Ion-Exchange experiments

The ion exchange properties of the produced PAN/Na-MMT composite nanofibers was evaluated by the following procedure: an aqueous solution of hexadecyltrimethylammonium bromide ($C_{16}TMA^+$ Br^- or $C_{16}TMABr$) [$CH_3(CH_2)_{15}N(Br)(CH_3)_3$ (Fluka, 25 wt%) (0.002 $mol.L^{-1}$) was prepared by dissolving 73 mg of $C_{16}TMABr$ powder in 100 ml distilled water in a volumetric flask. 70 mg of composite nanofibers filled with 5 wt% Na-MMT and produced at three different voltages (11.5, 13 and 14.5 kV) were dispersed in 10 mL of a 0.002 $mol.L^{-1}$ aqueous solution of $C_{16}TMABr$. After 2 h of stirring at room temperature, the solids were recovered by centrifugation at 15,000 rpm for 15 min before being oven-dried at 60°C for 12h. A blank was prepared in the same conditions starting from 20 mg of Na-MMT, these amount enables having the same content of sodium cations as in the PAN-Na-MMT composite samples. The obtained sample is labelled $C_{16}TMA$-MMT. XRD patterns of *001* plane of analyzed specimens were smoothed and base-line corrected using OriginPro 8 software.

3. Results and Discussion

3.1. Effect of incorporating Na-MMT on the thermal properties of composite nanofibers

It is known that PAN stabilization process takes place in an oxidative atmosphere [23]. A series of reactions occurs during the stabilization of PAN, which are

cyclization, dehydrogenation, aromatization, oxidation and crosslinking [24,25]. DTA curves of PAN and PAN/Na-MMT composite nanofibers (Figure 2) show that pristine PAN nanofibers exhibit an exothermic peak initiated at ca. 221 °C and centered at ca. 283 °C and that the loading of PAN with Na-MMT induces a shift of this peak toward higher temperature, with a temperature of 303°C for the sample loaded with 19 wt% of Na-MMT (

Table 1). This peak is attributed to the cyclization of nitrile groups of PAN [26]. These results suggest that the presence of Na-MMT imparts a higher thermal stability to PAN. The delay in PAN cyclization is likely due to the strong interaction between nitrile groups and Na-MMT aggregates.

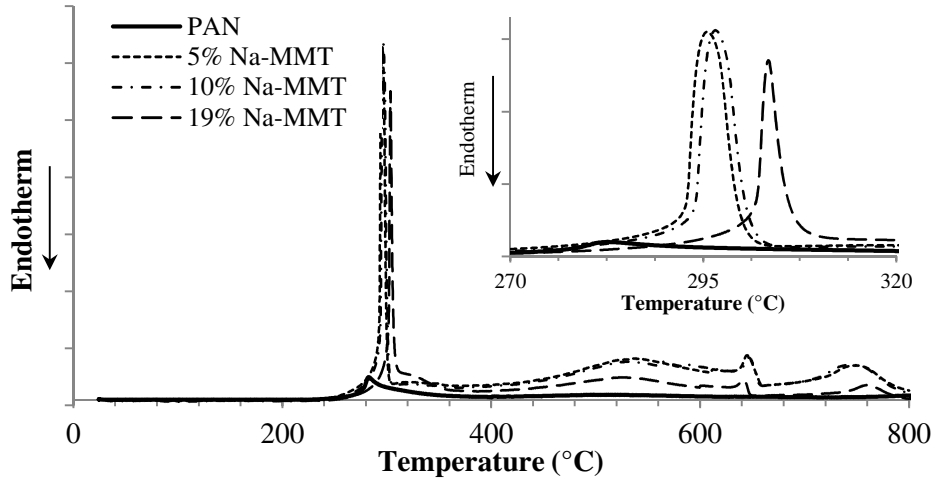

Figure 2 DTA curves of pristine PAN and PAN/Na-MMT composite nanofibers

(inset: DTA curves in the range of 270-320 °C)

Table 1 TGA-DTA results of PAN & PAN/Na-MMT nanofibers

Sample	**Exothermic peak**	

	Onset (°C)	Centered (°C)	**Mass loss (%)**
PAN	221	283	93
PAN+ 5 wt% Na-MMT	222	295	89
PAN+ 10 wt% Na-MMT	246	297	85
PAN+ 19 wt% Na-MMT	250	303	76

TGA thermograms (Figure 3) were simultaneously recorded with the DTA curves. These curves can be roughly divided into four parts (I, II, III and IV) regarding the extent of weight loss. The first part is up to 120 °C, in which all electrospun samples exhibit a significant initial weight loss corresponding to the desorption of the adsorbed water. Part II extends up to ca. 280 °C. Weight loss in this region is negligible and it corresponds to cyclization process since this latter does not cause theoretically any weight loss [27,28]. The third part is up to ca. 655 °C for PAN/Na-MMT composites and to ca. 800 °C for PAN nanofibers. The onset of this part implies a rapid weight loss for all samples arising from the dehydrogenation reaction [27]. Weight loss of PAN/Na-MMT composites is greater than that of pristine PAN. This is expected since Na-MMT was intercalated within PAN matrix leading to an interruption of polymer chain-chain interaction and therefore thermal degradation occurs easily. It is clear that the higher the loading percent of Na-MMT is, the lower the weight loss is, and the higher the onset temperature is in this region, too. In part IV, thermal degradation of PAN is terminated and Na-MMT with a ladder structure (i.e. a graphitic-like structure consisted of poly heterocyclic aromatic rings) are retained. Thermogravimetric analysis reveals that dispersions of PAN filled with 2, 3 and 5 wt% Na-MMT yield composite nanofibers loaded with 5, 10 and 19 wt% Na-MMT, respectively. The difference between loading percent determined from thermal analyses

and expected one indicates that PAN/Na-MMT suspensions are not stable and some Na-MMT particles have sedimented before electrospinning.

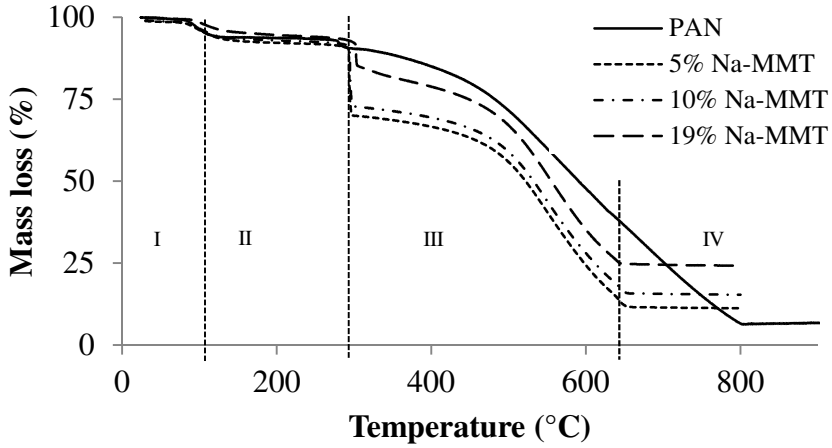

Figure 3 TGA curves of PAN and PAN/Na-MMT nanofibers

3.2. Effect of incorporating Na-MMT on the morphology of PAN/Na-MMT composite nanofibers

Erreur ! Source du renvoi introuvable. presents SEM micrographs of pristine PAN nanofibers and those produced from DMF solutions of PAN loaded with 5, 10 or 19 wt% Na-MMT. Pristine PAN nanofibers have diameters in the range of 600-700, 700-800 and 700-900 nm for applied voltages of 11.5, 13 and 14.5 kV, respectively. This indicates that the higher the applied voltage is, the coarser the nanofibers are. Typically, upon increasing the applied voltage, the ejected jet will be further electrified due to the increase in charges density carried on its surface. This augmentation in potential leads to an increase in the jet deposition velocity, i.e. a decreasing of the time that the jet would take to travel from the tip of the needle to the collector. Shorter travelling time would prevent the jet to be more stretched resulting in coarser nanofibers. These results are consistent with previous works [21,29,30].

As can be observed from Figure 4, Na-MMT aggregates are apparent along the nanofibers. Furthermore, the incorporation of Na-MMT into PAN matrix induces an increase the roughness of the produced composite nanofibers [20] and a decrease in the nanofibers average diameter with respect to their pristine counterparts, whatever the applied voltage is. It is worthy to note that there is a relationship between the nanofibers diameters and the Na-MMT content in the composite. Indeed, the higher the amount of Na-MMT in the composite is, the larger the diameter is [31] (Figure 5). In the case of sample electrospun at 13 kV, the average diameters of composite nanofibers filled with 5, 10 and 19 wt% Na-MMT, are 455±46, 583±50 and 717±49 nm, respectively, while the average diameter of pristine PAN is 747±29 nm.

Since Na-MMT has a high polarity arisen from its layer charges, it is thought that embedding Na-MMT into PAN matrix would increase the conductivity of the electrospun dispersion promoting therefore the production of finer nanofibers at higher voltages (all the other process parameters being constant) [19]. On the other hand, as the loading percent of Na-MMT increases, the diameter of produced nanofibers increases as well. It is assumed that nanofibers diameter is restricted by both the size and the mass fraction of Na-MMT aggregate, as already observed for PAN nonwovens charged by multi-walled carbon nanotubes [32] and by SBA-15 mesoporous silica [8].

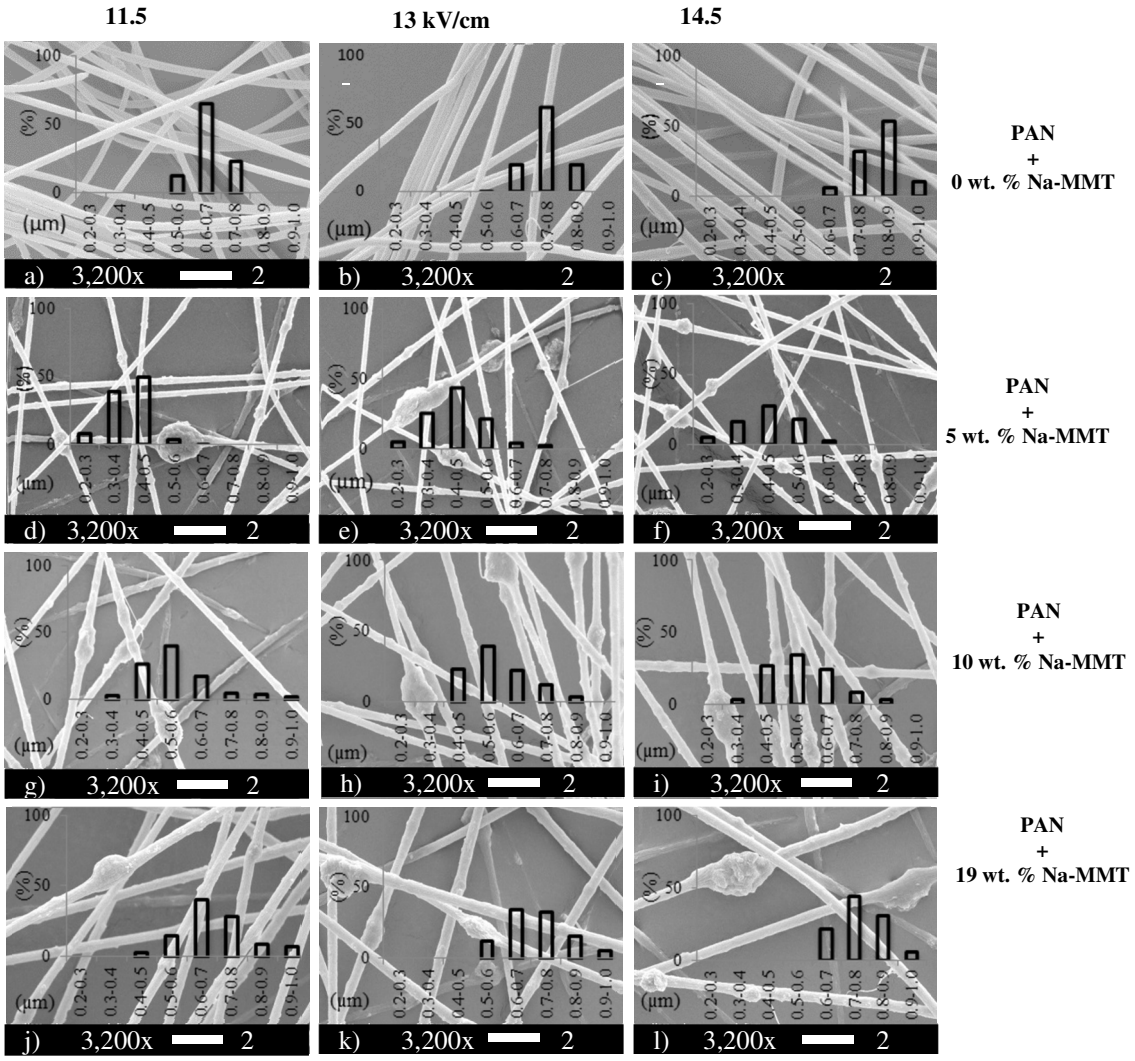

Figure 4 SEM micrographs and fiber diameter distribution of PAN nanofibers filled with Na-MMT particles

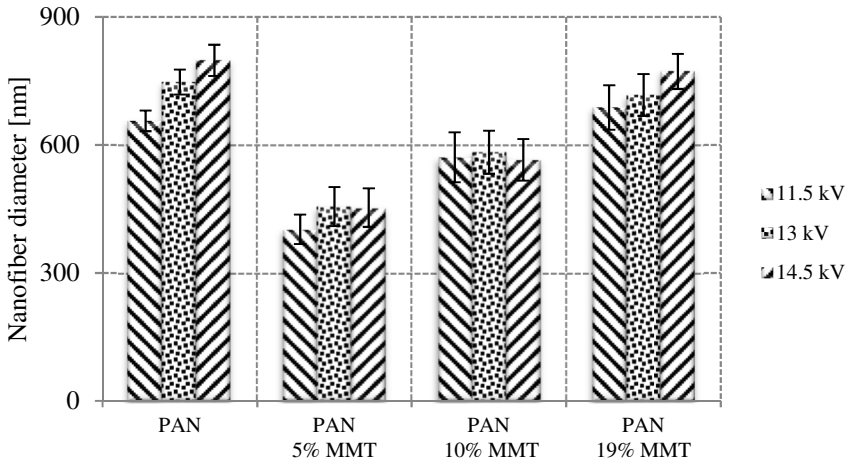

Figure 5 Nanofibers average diameter in relation to applied voltage.

3.3. Effect of incorporating Na-MMT within PAN nanofibers on Na-MMT structure

Na-MMT diffractogram (Figure 6) exhibits *hkl* bands at 4.45-4.48 Å (020, 110), 2.52-2.58 Å (130, 200), 1.67-1.70 Å (210) and 1.49 Å (060, 330) [33].

The first peak of Na-MMT diffractogram (2θ =7°) corresponds to (001) reflection. The position of this peak enables determining the d_{001} value and the basal spacing. This latter is the sum of the interlayer spacing and the thickness of the silicate layer (9.6 Å for montmorillonite [17,34]). Taking into account the d_{001} value of 12.7 Å for Na-MMT, the interlayer spacing of Na-MMT is found to be 3.1 Å.

Information about the nature of MMT platelet stacking can also be gathered from the shape of the (001) refelction. The more the 001 peak symmetric is, the more the platelets parallel are. In the case of neat Na-MMT, the first peak appears slightly asymmetric, indicating that the stacking of the platelets is not homogeneous.

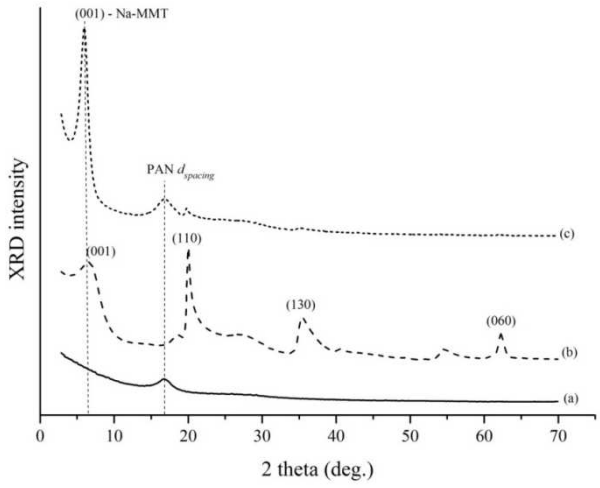

Figure 6 XRD patterns of PAN nanofibers (a), Na-MMT powder (b) and nanofibers of PAN filled with 19 wt% Na-MMT. (Nanofibers are produced at 11.5 kV)

PAN is a semi-crystalline polymer and exhibits a strong equatorial peak at 2Θ=16.8° in the wide angle X-ray diffraction pattern [35–37] corresponding to *d*-spacing equals to 5.8 Å.

PAN nanofibers filled with 19 wt% Na-MMT show diffraction peak at 2Θ=16.8° corresponding to PAN, and another peak at 2Θ=6° (d_{001}=14.8 Å) assigned to the reflection on the (001) plane of Na-MMT. The increase of the d_{001} value (14.8 Å compared to 12.7 Å for pristine Na-MMT) can be explained by the intercalation of PAN [38] or DMF [39,40] into Na-MMT gallery. This increase can also be due to the intercalation of water molecules present in the atmosphere.

Erreur ! Source du renvoi introuvable. summarizes XRD data of neat Na-MMT powder and PAN/Na-MMT composite nanofibers. These data reveal that whatever the applied voltage, the d_{001} value of Na-MMT in the composite is higher that the one of pristine Na-MMT. Skewness function is used to evaluate the degree of 001 peak asymmetry in each sample. It is worth to mention that positive values of skewness indicate a distribution with an asymmetric tail extending toward more positive values, and negative values indicate a distribution with an asymmetric tail extending toward more negative values.

Table 2 XRD data of PAN/Na-MMT composite nanofibers

Na-MMT 001 plane	Na-MMT powder	PAN/Na-MMT nanofibers					
		Produced at **13 kV** with different Na-MMT loadings (wt %)			filled with **19 wt%** Na-MMT and produced at different voltages (kV)		
		5	**10**	**19**	**11.5**	**13**	**14.5**
2Θ (°)	7.0	6.0	6.1	6.0	6.0	6.0	6.0
d_{001} (Å)	12.7	14.8	14.6	14.7	14.8	14.7	14.6
*Interlayer space (*Å)	3.1	5.2	5	5.1	5.2	5.1	5
Skewness	-1.02	-0.02	-0.22	-0.11	-0.25	-0.11	-0.10

As can be seen from Table 2, composite nanofibers electrospun with different loading percent of Na-MMT have smaller absolute values of skewness in comparison to neat Na-MMT powder. That means that the stacking of the Na-MMT layers is more homogenous in composite nanofibers. However, the loading percent has arbitrary influenced the degree of layers alignment to each other. Applied voltage improved layer alignment as can be concluded from skewness absolute values of composite nanofibers electrospun at different voltages. The higher the applied voltage is, the more ordered the layers stacking is.

3.4. Accessibility of Na-MMT interlayer space in PAN/Na-MMT composites

Figure 7 presents the X-ray diffractograms of neat Na-MMT powder, C_{16}TMA-MMT powder and PAN/Na-MMT samples as well as the C_{16}TMABr PAN/Na-MMT samples. A shift of the (001) reflexion toward a lower two theta angle (4.6°) is observed for all the C_{16}TMA-treated samples compared to the pristine samples (6.0°) corresponding to an increase of the basal spacing from 12.7 Å for Na-MMT to 19.7 Å for organically modified compounds. It can be concluded that sodium cations localized in the interlayer space are replaced by C_{16}TMA cations [41]. The shape of the (001) reflexions indicates an increase in the degree of coherent layer stacking, i.e. a more ordered organization of layered silicate within the organically treated composite nanofibres [42]. This indicates that the intercalation of alkylammonium ions into the clay gallery is still possible even after incorporating Na-MMT into PAN nanofibers. Accordingly, clay gallery is still accessible within the electrospun composite nanofibers.

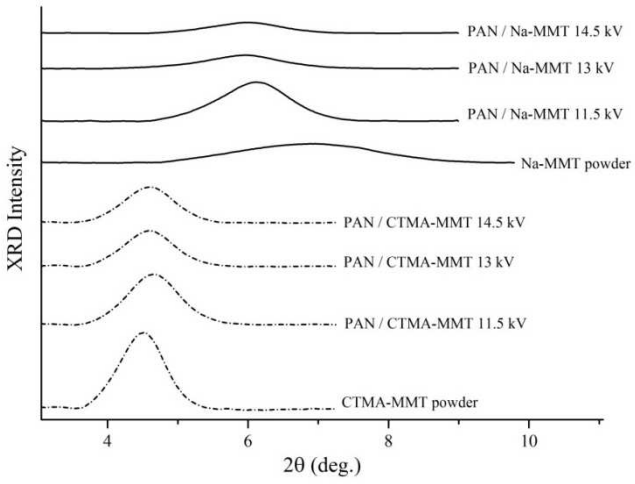

Figure 7 XRD patterns of pristine Na-MMTC16TMA-MMT, PAN/Na-MMT obtained at different voltages and C16TMA treated PAN/Na-MMT samples

4. Conclusions

Nonwovens of PAN/Na-MMT hybrid nanofibers containing 5, 10 or 19 wt% synthetic Na-MMT were produced by electrospinning PAN/Na-MMT/DMF solution at three different applied voltages; 11.5, 13 and 14.5 kV. Incorporating Na-MMT into PAN composite nanofibers induces an increase in the thermal stability of the hybrid nonwoven. This is evidenced by the shifting of exothermic peak of PAN toward higher temperature. A difference between the measured loading percents of Na-MMT within the composite nanofibers and those expected is marked indicating that PAN/Na-MMT suspensions are not stable and some Na-MMT particles have sedimented before electrospinning. A method to stabilize the electrospinning suspensions is envisaged.

SEM observations reveal that with increasing both Na-MMT and applied voltage, nanofiber diameter increases with a dominant influence of loading percent over that of applied voltage.

X-ray patterns of PAN/Na-MMT nanofibers indicate that Na-MMT incorporated within the nanofibers are intercalated by either PAN macromolecules, solvent molecules or by water molecules. This was confirmed by the shifting of the characteristic 001 peak of Na-

MMT into smaller 2θ values which correspond to an increase in the interlayer space from 12.7 Å for powder Na-MMT to 14.8 Å for incorporated Na-MMT. It was found that neither Na-MMT loading nor the applied voltage have a significant effect on the extent of silicate layer intercalation. However, the change in 001 peak skewness as a function of applied voltage confirms that the higher the applied voltage is, the more the layers parallel to each other are. In the limit of this study, no information can be confirmed concerning the alignment of Na-MMT layers to the axis of nanofiber. Observation by transmission electron microscopy will be envisaged for this purpose.

One interesting feature is that the interlayer space of Na-MMT is still accessible in the composite, applications in the field of environmental protection (waste water treatment, entrapping of organic pollutant) can therefore be expected. Studies are underway in order to tailor the Na-MMT dispersion and distribution in the nanofibers.

Further dispersing of Na-MMT silicate layers in the composite nanofibers is envisaged. Quantification of accessible galleries within the composite nanofibers will also be investigated.

5. References

[1] Yang F, Murugan R, Wang S, Ramakrishna S. Electrospinning of nano/micro scale poly(l-lactic acid) aligned fibers and their potential in neural tissue engineering. Biomaterials 2005;26:2603–10.

[2] Li D, Frey MW, Baeumner AJ. Electrospun polylactic acid nanofiber membranes as substrates for biosensor assemblies. Journal of Membrane Science 2006;279:354–63.

[3] Li M, Mondrinos MJ, Gandhi MR, Ko FK, Weiss AS, Lelkes PI. Electrospun protein fibers as matrices for tissue engineering. Biomaterials 2005;26:5999–6008.

[4] Hu X, Liu S, Zhou G, Huang Y, Xie Z, Jing X. Electrospinning of polymeric nanofibers for drug delivery applications. Journal of Controlled Release 2014;185:12–21.

[5] Lemma SM, Esposito A, Mason M, Brusetti L, Cesco S, Scampicchio M. Removal of bacteria and yeast in water and beer by nylon nanofibrous membranes. Journal of Food Engineering 2015;157:1–6.

[6] Mishra AK, Bose S, Kuila T, Kim NH, Lee JH. Silicate-based polymer-nanocomposite membranes for polymer electrolyte membrane fuel cells. Progress in Polymer Science n.d.

[7] Kim C, Ngoc BTN, Yang KS, Kojima M, Kim YA, Kim YJ, et al. Self-Sustained Thin Webs Consisting of Porous Carbon Nanofibers for Supercapacitors via the Electrospinning of Polyacrylonitrile Solutions Containing Zinc Chloride. Adv Mater 2007;19:2341–6.

[8] Almuhamed S, Khenoussi N, Bonne M, Schacher L, Lebeau B, Adolphe D, et al. Electrospinning of PAN nanofibers incorporating SBA-15-type ordered mesoporous silica particles. European Polymer Journal 2014;54:71–8.

[9] Jung H-R, Ju D-H, Lee W-J, Zhang X, Kotek R. Electrospun hydrophilic fumed silica/polyacrylonitrile nanofiber-based composite electrolyte membranes. Electrochimica Acta 2009;54:3630–7.

[10] Zhu J, Wei S, Rutman D, Haldolaarachchige N, Young DP, Guo Z. Magnetic polyacrylonitrile-Fe@FeO nanocomposite fibers - Electrospinning, stabilization and carbonization. Polymer 2011;52:2947–55.

[11] Sreekumar TV, Liu T, Min BG, Guo H, Kumar S, Hauge RH, et al. Polyacrylonitrile Single-Walled Carbon Nanotube Composite Fibers. Adv Mater 2004;16:58–61.

[12] Ji L, Zhang X. Ultrafine polyacrylonitrile/silica composite fibers via electrospinning. Materials Letters 2008; 62:2161–4.

[13] Chen J, Li Z, Chao D, Zhang W, Wang C. Synthesis of size-tunable metal nanoparticles based on polyacrylonitrile nanofibers enabled by electrospinning and microwave irradiation. Materials Letters 2008;62:692–4.

[14] Djenadic R, Winterer M. Chemical Vapor Synthesis of Nanocrystalline Oxides. Nanoparticles from the Gasphase, Springer Berlin Heidelberg; 2012, p. 49–76.

[15] Liu Z, Sakamoto Y, Ohsuna T, Hiraga K, Terasaki O, Ko CH, et al. TEM Studies of Platinum Nanowires Fabricated in Mesoporous Silica MCM-41. Angewandte Chemie International Edition 2000;39:3107–10.

[16] Balogh Z, Halasi G, Korbély B, Hernadi K. CVD-synthesis of multiwall carbon nanotubes over potassium-doped supported catalysts. Applied Catalysis A: General 2008;344:191–7.

[17] Ke YC, Stroeve P. Chapter 1 - Background on Polymer-Layered Silicate and Silica Nanocomposites. Polymer-Layered Silicate and Silica Nanocomposites, Amsterdam: Elsevier Science; 2005, p. 1–67.

[18] Saeed K, Park SY. Effect of nanoclay on the thermal, mechanical, and crystallization behavior of nanofiber webs of nylon-6. Polymer Composites 2012;33:192–5.

[19] Hong JH, Jeong EH, Lee HS, Baik DH, Seo SW, Youk JH. Electrospinning of polyurethane/organically modified montmorillonite nanocomposites. Journal of Polymer Science Part B: Polymer Physics 2005;43:3171–7.

[20] Li Q, Gao D, Wei Q, Ge M, Liu W, Wang L, et al. Thermal stability and crystalline of electrospun polyamide 6/organo-montmorillonite nanofibers. Journal of Applied Polymer Science 2010;117:1572–7.

[21] Lee HW, Karim MR, Ji HM, Choi JH, Ghim HD, Park SM, et al. Electrospinning fabrication and characterization of poly(vinyl alcohol)/montmorillonite nanofiber mats. Journal of Applied Polymer Science 2009;113:1860–7.

[22] Reinholdt M, Miehé-Brendlé J, Delmotte L, Tuilier M-H, le Dred R, Cortès R, et al. Fluorine Route Synthesis of Montmorillonites Containing Mg or Zn and Characterization by XRD, Thermal Analysis, MAS NMR, and EXAFS Spectroscopy. European Journal of Inorganic Chemistry 2001;2001:2831–41.

[23] Dalton S, Heatley F, Budd PM. Thermal stabilization of polyacrylonitrile fibres. Polymer 1999;40:5531–43.

[24] Rahaman MSA, Ismail AF, Mustafa A. A review of heat treatment on polyacrylonitrile fiber. Polymer Degradation and Stability 2007;92:1421–32.

[25] Bashir Z. A critical review of the stabilisation of polyacrylonitrile. Carbon 1991;29:1081–90.

[26] Peebles Jr. LH, Peyser P, Snow AW, Peters WC. On the exotherm of polyacrylonitrile: Pyrolysis of the homopolymer under inert conditions. Carbon 1990;28:707–15.

[27] Ouyang Q, Cheng L, Wang H, Li K. Mechanism and kinetics of the stabilization reactions of itaconic acid-modified polyacrylonitrile. Polymer Degradation and Stability 2008;93:1415–21.

[28] Xue TJ, McKinney MA, Wilkie CA. The thermal degradation of polyacrylonitrile. Polymer Degradation and Stability 1997;58:193–202.

[29] Chen M, Guo Z. Magnetic electrospun fluorescent polyvinylpyrrolidone nanocomposite fibers. Polymer 2012;53:4501–11.

[30] Atabey E, Wei S, Zhang X, Gu H, Yan X, Huang Y, et al. Fluorescent electrospun polyvinyl alcohol/CdSe@ZnS nanocomposite fibers. Journal of Composite Materials 2013;47:3175–85.

[31] Liu Y, Li C, Chen S, Wachtel E, Koga T, Sokolov JC, et al. Electrospinning of poly(ethylene-co-vinyl acetate)/clay nanocomposite fibers. Journal of Polymer Science Part B: Polymer Physics 2009;47:2501–8.

[32] Almuhamed S, Khenoussi N, Schacher L, Adolphe D, Balard H. Measuring of Electrical Properties of MWNT-Reinforced PAN Nanocomposites. Journal of Nanomaterials 2012;2012:7.

[33] Hofmann U, Maegdefrau E. Die Kristallstruktur des Montmorillonits. Zeitschrift Für Kristallographie - Crystalline Materials 1938;98. doi:10.1524/zkri.1938.98.1.299.

[34] Paul DR, Robeson LM. Polymer nanotechnology: Nanocomposites. Polymer 2008;49:3187–204.

[35] Bashir Z. Measurement of orientation in uniaxially drawn polyacrylonitrile. Acta Polymerica 1996;47:125–9.

[36] Davidson JA, Jung H-T, Hudson SD, Percec S. Investigation of molecular orientation in melt-spun high acrylonitrile fibers. Polymer 2000;41:3357–64.

[37] Fennessey SF, Farris RJ. Fabrication of aligned and molecularly oriented electrospun polyacrylonitrile nanofibers and the mechanical behavior of their twisted yarns. Polymer 2004;45:4217–25.

[38] Shami Z, Sharifi-Sanjani N. The role of Na-montmorillonite on thermal characteristics and morphology of electrospun PAN nanofibers. Fibers and Polymers 2010;11:695–9.

[39] Lagaly G. Characterization of clays by organic compounds. Clay Minerals 1981;16:1–21.

[40] Fong H, Liu W, Wang C-S, Vaia RA. Generation of electrospun fibers of nylon 6 and nylon 6-montmorillonite nanocomposite. Polymer 2002;43:775–80.

[41] Kooli F, Liu Y, Alshahateet SF, Messali M, Bergaya F. Reaction of acid activated montmorillonites with hexadecyl trimethylammonium bromide solution. Applied Clay Science 2009;43:357–63.

[42] Pavlidou S, Papaspyrides CD. A review on polymer–layered silicate nanocomposites. Progress in Polymer Science 2008;33:1119–98.